Field-Tunable Berezinskii-Kosterlitz-Thouless Correlations in a Heisenberg Magnet

D. Opherden,[1] M. S. J. Tepaske,[2,3] F. Bärtl,[1,4] M. Weber,[3] M. M. Turnbull,[5] T. Lancaster,[6] S. J. Blundell,[7] M. Baenitz,[8] J. Wosnitza,[1,4] C. P. Landee,[9] R. Moessner,[3] D. J. Luitz,[2,3] and H. Kühne[1,*]

[1]*Hochfeld-Magnetlabor Dresden (HLD-EMFL) and Würzburg-Dresden Cluster of Excellence ct.qmat, Helmholtz-Zentrum Dresden-Rossendorf, 01328 Dresden, Germany*
[2]*Physikalisches Institut, Universität Bonn, Nussallee 12, 53115 Bonn, Germany*
[3]*Max Planck Institute for the Physics of Complex Systems, 01187 Dresden, Germany*
[4]*Institut für Festkörper- und Materialphysik, TU Dresden, 01062 Dresden, Germany*
[5]*Carlson School of Chemistry, Clark University, Worcester, Massachusetts 01610, USA*
[6]*Department of Physics, Centre for Materials Physics, Durham University, Durham DH1 3LE, United Kingdom*
[7]*Clarendon Laboratory, Department of Physics, University of Oxford, Park Road, Oxford OX1 3PU, United Kingdom*
[8]*Max Planck Institute for Chemical Physics of Solids, 01187 Dresden, Germany*
[9]*Department of Physics, Clark University, Worcester, Massachusetts 01610, USA*

(Received 14 September 2022; accepted 18 January 2023; published 23 February 2023)

We report the manifestation of field-induced Berezinskii-Kosterlitz-Thouless (BKT) correlations in the weakly coupled spin-1/2 Heisenberg layers of the molecular-based bulk material $[Cu(pz)_2(2\text{-}HOpy)_2](PF_6)_2$. At zero field, a transition to long-range order occurs at 1.38 K, caused by a weak intrinsic easy-plane anisotropy and an interlayer exchange of $J'/k_B \approx 1$ mK. Because of the moderate intralayer exchange coupling of $J/k_B = 6.8$ K, the application of laboratory magnetic fields induces a substantial XY anisotropy of the spin correlations. Crucially, this provides a significant BKT regime, as the tiny interlayer exchange J' only induces 3D correlations upon close approach to the BKT transition with its exponential growth in the spin-correlation length. We employ nuclear magnetic resonance measurements to probe the spin correlations that determine the critical temperatures of the BKT transition as well as that of the onset of long-range order. Further, we perform stochastic series expansion quantum Monte Carlo simulations based on the experimentally determined model parameters. Finite-size scaling of the in-plane spin stiffness yields excellent agreement of critical temperatures between theory and experiment, providing clear evidence that the nonmonotonic magnetic phase diagram of $[Cu(pz)_2(2\text{-}HOpy)_2](PF_6)_2$ is determined by the field-tuned XY anisotropy and the concomitant BKT physics.

DOI: 10.1103/PhysRevLett.130.086704

Cooperative behavior and critical phenomena of strongly correlated magnets are typically dictated by the lattice and spin dimensions, as well as by the symmetry of the underlying Hamiltonian [1–8]. Among the most fascinating examples are two-dimensional (2D) XY spin systems, which are known to undergo a topological Berezinskii-Kosterlitz-Thouless phase transition at a finite temperature T_{BKT} [9–11], which marks the binding of topological defects in vortex-antivortex pairs. So far, experimental efforts to probe a genuine BKT transition in a bulk material were compromised by the onset of 3D order [12–18] due to the inherent 3D nature of these materials. Still, if the perturbative terms relative to a purely 2D XY model are small enough, the experimental observation of magnetic properties associated with BKT correlations may be possible in the transition regime [19–23].

In particular, a controlled tuning of the XY anisotropy, with associated impact on T_{BKT}, can provide an ideal test bed for experimental studies of BKT physics and their comparison to numerical state-of-the-art modeling. As a possible approach to tune the magnetic correlations away from 2D Heisenberg to a 2D XY symmetry, the application of a uniform magnetic field to the 2D quantum Heisenberg antiferromagnet breaks the $O(3)$ symmetry, but preserves the easy-plane $O(2)$ symmetry, as was confirmed by quantum Monte Carlo (QMC) calculations [24]. Correspondingly, for Zeeman energies of the order of the exchange energy, the effective XY-exchange anisotropy can be controlled. The associated BKT transition persists for all fields below saturation, yielding a nonmonotonic magnetic phase diagram [24].

In order to find materials that allow us to study this phenomenology, the chemical engineering of molecular-based bulk magnets is a promising approach. By an appropriate choice of molecular ligands and counterions, the syntheses of several materials that realize a 2D spin-1/2 Heisenberg model on the square lattice were reported [25–35]. In these materials, a moderate

nearest-neighbor exchange interaction of the order of a few K allows for the tunability of the effective exchange anisotropy by experimentally accessible magnetic fields. Indeed, for several Cu^{2+}-based molecular materials, a nonmonotonic magnetic phase diagram as a function of the external field was reported [25,30,32,36,37]. The magnetic properties of these molecular-based 2D quantum Heisenberg antiferromagnets were mostly investigated by thermodynamic methods [26,30,32,34,35], thus missing local information about the magnetic correlations in the BKT transition regime.

In this Letter, we report on the field-tunable anisotropy of magnetic correlations in $[Cu(pz)_2(2\text{-}HOpy)_2](PF_6)_2$ [with $pz = C_4H_4N_2$, $2\text{-}HOpy = C_5H_4NHO$] (CuPOF in the following), ranging from the almost-isotropic Heisenberg limit at zero field to a substantial XY anisotropy upon increasing the magnetic field strength. We use nuclear magnetic resonance (NMR) as the experimental probe for the dynamic and quasistatic spin correlations. Furthermore, by QMC simulations, we calculate the in-plane spin stiffness, which we use to determine the critical temperatures of the long-range order (LRO) and the BKT transition. Our main findings are (i) that the temperature dependence of the nuclear spin-lattice relaxation rate follows the behavior predicted from 2D BKT theory in a wide range of temperatures, determined by the field-driven anisotropy, (ii) that finite-size scaling of the QMC results permits the extraction of T_{BKT}, which lies below the actual 3D ordering temperature T_{LRO}, and (iii) that both temperatures exhibit a nonmonotonic field dependence, which is analogous to the behavior when instead of the field, the anisotropy of interactions is tuned, a clear signature for the tunability of BKT correlations.

The synthesis and characterization of CuPOF by means of various techniques, including μ^+SR experiments, are described in Ref. [25]. The crystals are flat plates with the crystallographic c axis perpendicular to the plate. The NMR spectra and spin-lattice relaxation time T_1 were recorded using a standard Hahn spin-echo pulse sequence and an inversion-recovery method, respectively. The measurements were performed using a commercial phase-coherent spectrometer and a 16 T superconducting magnet, equipped with a ^{3}He sample-in-liquid cryostat. A single-axis goniometer was used to align the c axis parallel to the magnetic field.

The magnetic interactions of CuPOF in an applied field are well approximated by the effective Hamiltonian

$$\mathcal{H} = J\sum_{\langle i,j\rangle_{\parallel}}[S_i^xS_j^x + S_i^yS_j^y + (1-\Delta)S_i^zS_j^z] + J'\sum_{\langle i,j\rangle_{\perp}}\mathbf{S}_i\cdot\mathbf{S}_j - g\mu_B\mu_0H\sum_i S_i^z, \quad (1)$$

where $\langle i,j\rangle_{\parallel}$ and $\langle i,j\rangle_{\perp}$ denote the intra- and interlayer nearest neighbors, and J and J' are the intra- and interlayer exchange couplings, estimated as $J/k_B = 6.8$ K and $J'/k_B \approx 1$ mK [25]. Whereas $\Delta = 0$ corresponds to the isotropic Heisenberg case, $0 < \Delta \leq 1$ quantifies an easy-plane anisotropy, with a zero-field value of $\Delta \approx 0.01\ldots0.02$ for CuPOF [25].

In the presence of interlayer interactions, any nonfrustrated magnetic quasi-2D lattice inevitably undergoes a transition to long-range order at low temperatures. Because of the very large separation of the magnetic layers in CuPOF, with $J'/J \approx 1.4\times10^{-4}$, the very small entropy change associated with the transition to LRO is beyond the experimental resolution of thermodynamic quantities [25,38]. On the other hand, μ^+SR is very sensitive to the local staggered magnetization, and was used to probe the transition to LRO at 1.38 (2) K in CuPOF [25]. This transition occurs under the influence of the weak intrinsic easy-plane anisotropy, which yields a temperature-driven crossover from isotropic to XY-type correlations at the crossover temperature $T_{\mathrm{co}} > T_{\mathrm{LRO}}$. An applied magnetic field increases the effective XY anisotropy, which manifests itself as a field-dependent minimum of the uniform bulk susceptibility at T_{co}, as depicted by the pentagons in Fig. 1.

The temperature dependence of the ^{31}P-NMR spin-lattice relaxation rate at out-of-plane fields up to 16 T is presented

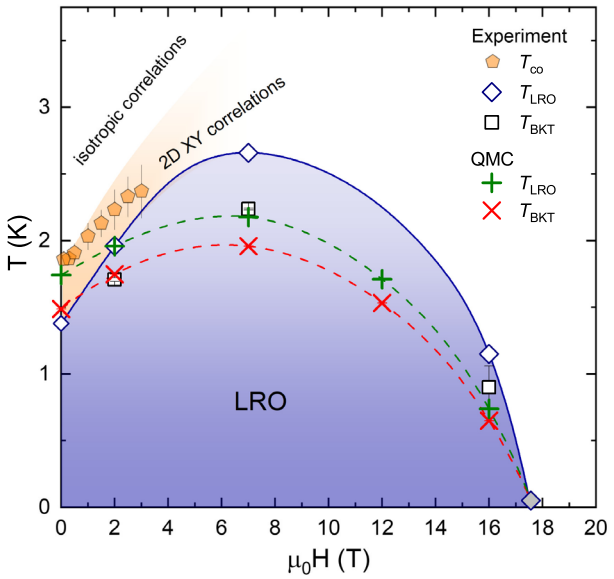

FIG. 1. Phase diagram of CuPOF for out-of-plane magnetic fields from experiment and numerics. The pentagons denote the spin-anisotropy crossover temperature T_{co} from Ref. [25]. White diamonds indicate the transition temperature T_{LRO} to long-range order, and squares show the BKT transition temperature T_{BKT}, as obtained from the analysis of the ^{31}P $1/T_1$ rate (Fig. 2). T_{LRO} at zero field is determined by μ^+SR measurements [25]. The green pluses and red crosses denote T_{LRO} and T_{BKT}, respectively, as obtained from QMC calculations (Fig. 3). The diamond at 17.5 T denotes the saturation field, which was determined from magnetization experiments [25], and is in agreement with QMC results. All lines are guides to the eye.

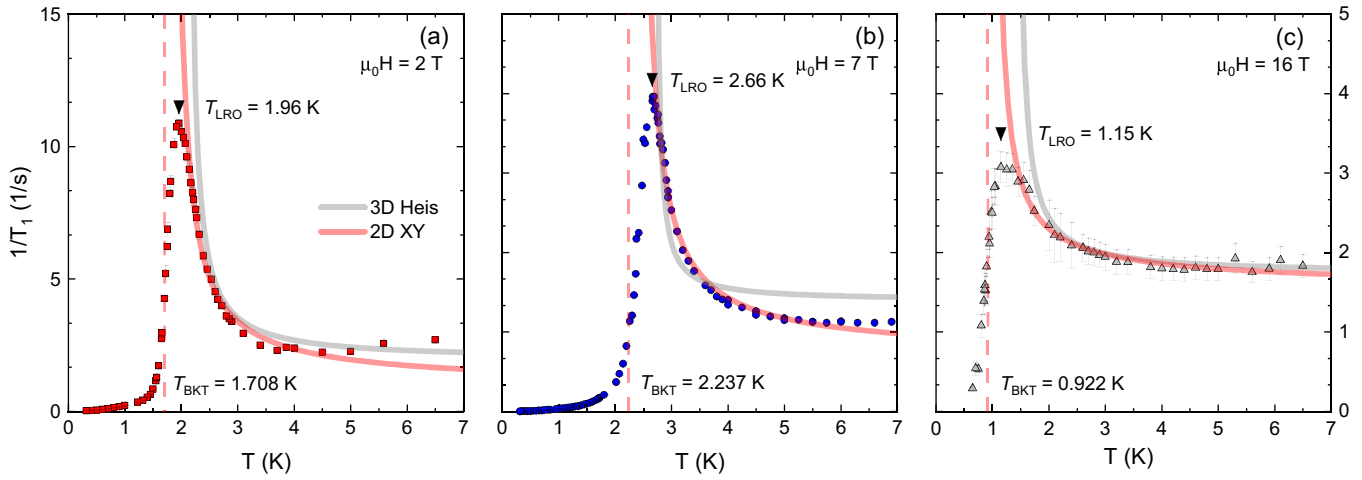

FIG. 2. (a)–(c) Temperature-dependent ^{31}P nuclear spin-lattice relaxation rate $1/T_1$ of CuPOF, recorded at out-of-plane fields of 2, 7, and 16 T. The solid lines are best fits according to $1/T_1 \propto \xi^{z-\eta}$ for the temperature dependent correlation lengths $\xi_{3\mathrm{DHeis}}$ and $\xi_{2\mathrm{DXY}}$ of the 3D Heisenberg and the 2D XY cases (see main text). The transition temperature T_{LRO}, marked with a downward triangle, is inferred from the $1/T_1$ peak position, and T_{BKT}, marked with a dotted line, is determined from fits according to $1/T_1 \propto \xi_{2\mathrm{DXY}}^{z-\eta}$. At all fields, but most noticeably at 7 T, $1/T_1$ is described best by $\xi_{2\mathrm{DXY}}$ at $T \gtrsim T_{\mathrm{LRO}}$.

in Figs. 2(a)–2(c). The spin-lattice relaxation rate $1/T_1$ has sharp maxima at $T_{\mathrm{LRO}} = 1.96$ and 2.66 K at 2 and 7 T, respectively. In comparison, the maximum amplitude of $1/T_1$ at 16 T ($T_{\mathrm{LRO}} = 1.15$ K) is substantially reduced. The transition temperatures between the 2D XY and the LRO regimes are depicted by diamonds in Fig. 1. The strong dependence of T_{LRO} on the field strength that we observe in CuPOF clearly indicates a field tunability of the XY anisotropy of the spin correlations [24]. This behavior is confirmed by our QMC simulations.

As previously reported, the ^{31}P $1/T_1$ rate in CuPOF yields several broad maxima at high temperatures, which are associated with a freezing of the PF_6 molecular reorientation modes [39]. Below about 10 K, in the range of interest in the present study, these modes are frozen out and $1/T_1$ becomes temperature independent, indicating predominantly paramagnetic fluctuations. In 2D magnetic lattices, the onset of short-range spin correlations occurs at temperatures $T \simeq J/k_B$ [38], with a correlation length of about one magnetic-lattice constant [16,40].

At temperatures above the onset of LRO, $1/T_1$ can serve as a probe for the dynamic correlation length ξ [19,20,41–44]. As was shown from dynamical scaling arguments [41], $1/T_1$ is proportional to the transverse spin correlation length as $1/T_1 \propto \xi^{z-\eta}$, where z and η are characteristic dynamic and critical exponents [3,19,41,45]. By comparing the temperature dependence of $1/T_1$ with the characteristic ξ of different universality classes, we can therefore probe the nature of the predominant correlations in the critical regime, before the system finally undergoes the transition to long-range order. Thus, we compare the BKT correlation length of a 2D easy-plane antiferromagnet, $\xi_{2\mathrm{DXY}} \propto \exp(0.5\pi/\sqrt{T/T_{\mathrm{BKT}} - 1})$ [11,16], with that of a 3D isotropic Heisenberg antiferromagnet, $\xi_{3\mathrm{DHeis}} \propto |T - T_{\mathrm{LRO}}|^{-0.7112}$ [46,47].

To describe $1/T_1$ in the interval $T_{\mathrm{LRO}} \leq T \leq J/k_B$, we note that $\eta = 0.0375$ for the 3D Heisenberg antiferromagnet [46], with the LRO transition residing in the $O(3)$ universality class, whereas the easy-plane model has $\eta = 1/4$ [48–50]. For both models, we use $z = d/2$, with d the spatial dimensionality [45]. The experimental estimates of T_{BKT} are obtained from fits to the 2D XY form.

In Figs. 2(a)–2(c), we show the measured $1/T_1$ along with both fits, for fields of 2, 7, and 16 T [51]. In contrast to the 3D Heisenberg description, the 2D XY fit accurately captures the increase of $1/T_1$ near T_{LRO}, most noticeably at 7 T. The fits yield $T_{\mathrm{BKT}} = 1.708(14)$, 2.237(7), and 0.90(16) K for applied fields of 2, 7, and 16 T, respectively, with errors determined by bootstrapping. The nonmonotonic dependence of T_{BKT} on the field tracks that of T_{LRO}, being separated by a few hundred mK for the most part, as shown in the phase diagram in Fig. 1. One should note, however, that the BKT transition is preempted by the LRO that arises from the 3D correlations, stemming from the finite interlayer exchange interaction J'. In the Supplemental Material [52], we discuss indications that changing the field strength has similar effects on the spin correlations as changing the exchange anisotropy Δ [16,62] and argue that hence the field allows us to tune the effective anisotropy. Further, as shown by μ^+SR and ^{1}H-NMR spectroscopy, the low-temperature staggered magnetization in CuPOF agrees with a change from Heisenberg behavior at zero field towards that of a 2D XY system at 7 T, see Fig. S2 in the Supplemental Material [52].

In order to shed more light on the experimentally observed phenomenology of mixed Néel and BKT-type

correlations, we numerically investigate the Hamiltonian (1) using stochastic series expansion quantum Monte Carlo with directed loops [63]. We consider finite simple-cubic lattices with periodic boundary conditions and dimensions $L \times L \times L/8$, fixing $J/k_B = 6.8$ K, $J'/k_B = 1$ mK, and $\Delta = 0.0185$. To determine T_{BKT} and T_{LRO}, we calculate the in-plane spin stiffness $\rho = 8L^{-3}\partial^2 F/\partial\phi^2|_{\phi=0}$, which is defined as the second derivative of the free energy F with respect to a uniform in-plane twist angle ϕ [64,65]. This quantity is nonzero in the BKT phase and in the thermodynamic limit it should vanish instantly at T_{BKT}. For the finite lattices simulated with QMC, this drop-off is instead continuous, but based on how ρ approaches the instant drop-off with increasing system size, we can determine T_{BKT}. In particular, using finite-size scaling theory, it is predicted that ρ depends on temperature T and system size L as [64]

$$\rho(T,L)/P(L) = f\left(\ln(L) - \frac{a}{\sqrt{T - T_{\mathrm{BKT}}}}\right), \quad (2)$$

$$P(L) = 1 + \frac{1}{2\ln(L) + c + \ln[c/2 + \ln L]} + \frac{b}{\ln^2 L}, \quad (3)$$

where a, b, c are fitting constants and f is a general continuous function which we choose to be a fifth-order polynomial. This parametrization of ρ is fitted closely above T_{BKT} for simulation data of the $J' = 0$ model to deduce T_{BKT}. Afterwards, we plot ρ/P versus $\ln(L) - a/\sqrt{T - T_{\mathrm{BKT}}}$ in the fitting interval, which should collapse to a single curve if the fit is perfect. We checked that fitting ρ for $J' = 1$ mK in the full 3D model reproduces the 2D T_{BKT} to within error bars, when fitted at $T > T_{\mathrm{LRO}}$, where the interlayer coupling becomes insignificant such that the 2D scaling ansatz (3) holds. In Fig. 3(a), we show the finite-size collapse of the ρ fit performed at 2 T, for systems with up to 1×10^6 spins and a temperature grid of $\Delta T = 1$ mK. The fit yields $T_{\mathrm{BKT}} = 1.748(15)$ K.

To determine T_{LRO}, we consider the scaled in-plane stiffness $L\rho$ for the full 3D model with $J' = 1$ mK. At large L, this quantity becomes size independent at T_{LRO} [47]. Hence, by determining the crossings T^* between $L\rho$ curves with two different sizes L, and extrapolating this crossing temperature to $L \to \infty$, we obtain T_{LRO} [66]. In Fig. 3(b), we show the scaling analysis performed for $L\rho$ at 2 T, where the inset shows the $L \to \infty$ scaling of the crossing temperature T^*. Here, we used a second-order polynomial, which yields $T_{\mathrm{LRO}} = 1.959(2)$ K. Further calculations of the relevant magnetization components and correlation length are presented in Fig. S3 of the Supplemental Material [52].

Employing these procedures at different magnetic fields, we determined $T_{\mathrm{BKT}} = 1.4877(6)$, 1.7477(15), 1.9584(24), 1.5323(13), and 0.6495(15) K, at fields of 0, 2, 7, 12, and 16 T, respectively. We also confirmed that $T_{\mathrm{BKT}} = 0$ when both $\Delta = 0$ and $H = 0$, which emphasizes the strong effect

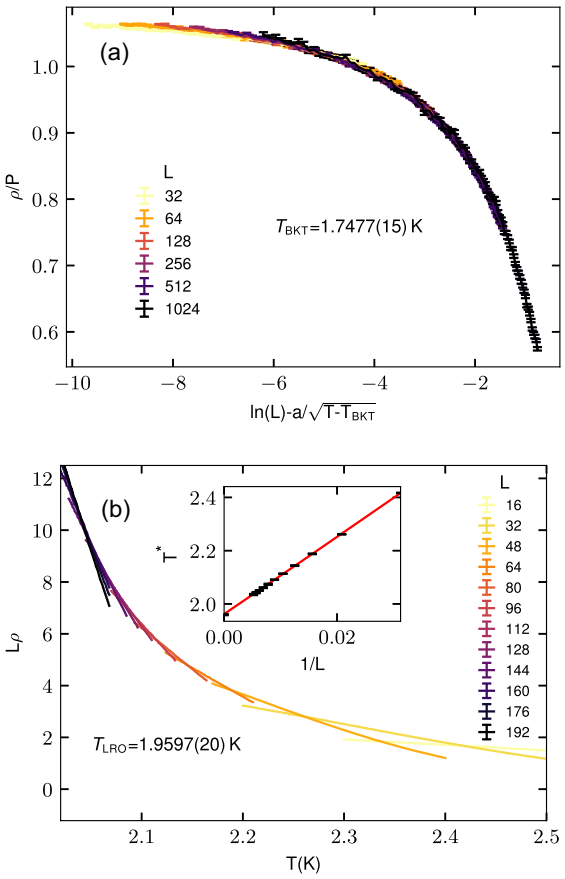

FIG. 3. Finite-size scaling analysis performed to obtain the critical temperatures T_{BKT} and T_{LRO} from the QMC simulations at 2 T. (a) Data collapse of the finite-size in-plane spin stiffness ρ fit closely above T_{BKT}, for the $J' = 0$ model, which should collapse to a single curve if the fit is perfect, reaffirming the calculated T_{BKT}. The different curves correspond to different linear sizes L. (b) Crossings of the $L\rho$ curves for the $J' = 1$ mK model; the inset shows the $L \to \infty$ scaling of the crossing temperature T^*. The red line denotes a second-order polynomial fit, which is extrapolated to $1/L \to 0$ to estimate T_{LRO}.

on T_{BKT} of the seemingly small $\Delta = 0.0185$ for CuPOF. Furthermore, we determined $T_{\mathrm{LRO}} = 1.7425(19)$, 1.9597 (20), 2.1768(23), 1.7110(22), and 0.7376(17) K. At all fields, our calculations yield $T_{\mathrm{LRO}} > T_{\mathrm{BKT}}$, thus supporting the experimental phenomenology, as can be seen in Fig. 1. We also determined the saturation field to be 17.5 T, in excellent agreement with the experimental value. As in the experiment, the strong dependence of the numerically determined T_{LRO} on the field strength reflects the effect of the field-induced anisotropy. The quantitative differences to the experimental transition temperatures at elevated fields might be resolved by extending the complexity of the modelling. In Fig. S4 of the Supplemental Material, we obtain a simple estimate of an effective exchange anisotropy $\Delta(H)$ at $H \leq 6$ T and compare it to the low-field results [52].

Our findings suggest the following scenario for the temperature evolution of spin correlations in CuPOF in applied magnetic fields. Decreasing the temperatures from the paramagnetic high-temperature limit, isotropic Heisenberg-type spin correlations develop, which cross over to an anisotropic XY-type close to T_{co}. With further decreasing temperature, the correlation length ξ grows exponentially due to the vortex physics described by BKT theory. For $T \gtrsim T_{BKT}$, a rather low density of these topological excitations is expected [67]. The exponential increase of ξ yields a rapid strengthening of the antiferromagnetic correlations in the XY regime and, therefore, the staggered magnetization appears effectively nonzero even above T_{LRO} (see Supplemental Material) [52]. With further increase of ξ upon lowering the temperature further, the magnetic correlations, due to the influence of the small but nonzero interlayer interaction J' on the regions with large in-plane correlation lengths, can no longer be treated as 2D, and a transition to long-range order occurs at T_{LRO}. As a consequence of the field-induced BKT-type spin correlations, a concomitant nonmonotonic behavior of the transition temperature T_{LRO} is observed experimentally and confirmed by our QMC simulations.

In conclusion, the very good agreement between our experimental results and the matching QMC calculations establishes our study of CuPOF as a model case, where the application of a magnetic field allows a controlled tuning of the spin-1/2 system from the almost isotropic 2D Heisenberg to the highly anisotropic 2D XY limit. The phenomenology in CuPOF is driven by field-induced Berezinskii-Kosterlitz-Thouless physics under the influence of extremely small interplane interactions, thus providing an attractive opportunity for systematic investigations of the BKT-type topological excitations and calling for further experimental studies by inelastic scattering techniques.

Data presented in this Letter resulting from the UK effort are available from [68].

We acknowledge the support of HLD at HZDR, a member of the European Magnetic Field Laboratory (EMFL). This work was supported by the Deutsche Forschungsgemeinschaft (DFG) through SFB 1143 (project ID 247310070), the Würzburg-Dresden Cluster of Excellence on Complexity and Topology in Quantum Matter—*ct.qmat* (EXC 2147, project ID 390858490) and the cluster of excellence ML4Q (EXC2004, project ID 390534769). Our QMC code is based on the ALPS libraries [69]. Part of this work was carried out at the STFC ISIS facility and we are grateful for provision of beam time. This work is supported by EPSRC (UK).

D. O. and M. S. J. T. contributed equally to this work.

*Corresponding author.
h.kuehne@hzdr.de

[1] L. Onsager, Phys. Rev. **65**, 117 (1944).
[2] N. D. Mermin and H. Wagner, Phys. Rev. Lett. **17**, 1133 (1966).
[3] *Magnetic Properties of Layered Transition Metal Compounds*, edited by L. J. d. Jongh (Springer, Netherlands, 1990).
[4] B. Widom, J. Chem. Phys. **43**, 3898 (1965).
[5] M. E. Fisher, Rev. Mod. Phys. **46**, 597 (1974).
[6] K. G. Wilson, Rev. Mod. Phys. **47**, 773 (1975).
[7] M. J. Feigenbaum, Physica (Amsterdam) **7D**, 16 (1983).
[8] P. W. Anderson, Science **235**, 1196 (1987).
[9] V. L. Berezinskii, J. Exp. Theor. Phys. **32**, 493 (1971).
[10] J. M. Kosterlitz and D. J. Thouless, J. Phys. C **6**, 1181 (1973).
[11] J. M. Kosterlitz, J. Phys. Condens. Matter **7**, 1046 (1974).
[12] B.-G. Liu, Phys. Rev. B **41**, 9563 (1990).
[13] N. Majlis, S. Selzer, and G. C. Strinati, Phys. Rev. B **45**, 7872 (1992).
[14] N. Majlis, S. Selzer, and G. C. Strinati, Phys. Rev. B **48**, 957 (1993).
[15] L. Siurakshina, D. Ihle, and R. Hayn, Phys. Rev. B **61**, 14601 (2000).
[16] H.-Q. Ding, Phys. Rev. Lett. **68**, 1927 (1992).
[17] H.-Q. Ding, J. Phys. Condens. Matter **2**, 7979 (1990).
[18] A. Cuccoli, T. Roscilde, R. Vaia, and P. Verrucchi, Phys. Rev. Lett. **90**, 167205 (2003).
[19] B. J. Suh, F. Borsa, L. L. Miller, M. Corti, D. C. Johnston, and D. R. Torgeson, Phys. Rev. Lett. **75**, 2212 (1995).
[20] D. Waibel, G. Fischer, T. Wolf, H. v. Löhneysen, and B. Pilawa, Phys. Rev. B **91**, 214412 (2015).
[21] E. S. Klyushina, J. Reuther, L. Weber, A. T. M. N. Islam, J. S. Lord, B. Klemke, M. Må nsson, S. Wessel, and B. Lake, Phys. Rev. B **104**, 064402 (2021).
[22] N. Caci, L. Weber, and S. Wessel, Phys. Rev. B **104**, 155139 (2021).
[23] P. Carretta, M. Filibian, R. Nath, C. Geibel, and P. J. C. King, Phys. Rev. B **79**, 224432 (2009).
[24] A. Cuccoli, T. Roscilde, R. Vaia, and P. Verrucchi, Phys. Rev. B **68**, 060402(R) (2003).
[25] D. Opherden *et al.*, Phys. Rev. B **102**, 064431 (2020).
[26] F. M. Woodward, P. J. Gibson, G. B. Jameson, C. P. Landee, M. M. Turnbull, and R. D. Willett, Inorg. Chem. **46**, 4256 (2007).
[27] P. A. Goddard, J. Singleton, P. Sengupta, R. D. McDonald, T. Lancaster, S. J. Blundell, F. L. Pratt, S. Cox, N. Harrison, J. L. Manson, H. I. Southerland, and J. A. Schlueter, New J. Phys. **10**, 083025 (2008).
[28] F. Xiao, F. M. Woodward, C. P. Landee, M. M. Turnbull, C. Mielke, N. Harrison, T. Lancaster, S. J. Blundell, P. J. Baker, P. Babkevich, and F. L. Pratt, Phys. Rev. B **79**, 134412 (2009).
[29] J. L. Manson, K. H. Stone, H. I. Southerland, T. Lancaster, A. J. Steele, S. J. Blundell, F. L. Pratt, P. J. Baker, R. D. McDonald, P. Sengupta, J. Singleton, P. A. Goddard, C. Lee, M.-H. Whangbo, M. M. Warter, C. H. Mielke, and P. W. Stephens, J. Am. Chem. Soc. **131**, 4590 (2009).
[30] E. Čižmár, S. A. Zvyagin, R. Beyer, M. Uhlarz, M. Ozerov, Y. Skourski, J. L. Manson, J. A. Schlueter, and J. Wosnitza, Phys. Rev. B **81**, 064422 (2010).

[31] A. J. Steele, T. Lancaster, S. J. Blundell, P. J. Baker, F. L. Pratt, C. Baines, M. M. Conner, H. I. Southerland, J. L. Manson, and J. A. Schlueter, Phys. Rev. B **84**, 064412 (2011).

[32] Y. Kohama, M. Jaime, O. E. Ayala-Valenzuela, R. D. McDonald, E. D. Mun, J. F. Corbey, and J. L. Manson, Phys. Rev. B **84**, 184402 (2011).

[33] P. A. Goddard, J. L. Manson, J. Singleton, I. Franke, T. Lancaster, A. J. Steele, S. J. Blundell, C. Baines, F. L. Pratt, R. D. McDonald, O. E. Ayala-Valenzuela, J. F. Corbey, H. I. Southerland, P. Sengupta, and J. A. Schlueter, Phys. Rev. Lett. **108**, 077208 (2012).

[34] P. A. Goddard *et al.*, Phys. Rev. B **93**, 094430 (2016).

[35] V. Selmani, C. P. Landee, M. M. Turnbull, J. L. Wikaira, and F. Xiao, Inorg. Chem. Commun. **13**, 1399 (2010).

[36] P. Sengupta, C. D. Batista, R. D. McDonald, S. Cox, J. Singleton, L. Huang, T. P. Papageorgiou, O. Ignatchik, T. Herrmannsdörfer, J. L. Manson, J. A. Schlueter, K. A. Funk, and J. Wosnitza, Phys. Rev. B **79**, 060409(R) (2009).

[37] N. A. Fortune, S. T. Hannahs, C. P. Landee, M. M. Turnbull, and F. Xiao, J. Phys. Conf. Ser. **568**, 042004 (2014).

[38] P. Sengupta, A. W. Sandvik, and R. R. P. Singh, Phys. Rev. B **68**, 094423 (2003).

[39] D. Opherden, F. Bärtl, S. Yamamoto, Z. T. Zhang, S. Luther, S. Molatta, J. Wosnitza, M. Baenitz, I. Heinmaa, R. Stern, C. P. Landee, and H. Kühne, Phys. Rev. B **103**, 014428 (2021).

[40] H.-Q. Ding and M. S. Makivić, Phys. Rev. Lett. **64**, 1449 (1990).

[41] F. Borsa, M. Corti, T. Goto, A. Rigamonti, D. C. Johnston, and F. C. Chou, Phys. Rev. B **45**, 5756 (1992).

[42] F. Tabak, A. Lascialfari, and A. Rigamonti, J. Phys. Condens. Matter **5**, B31 (1993).

[43] L. Bossoni, P. Carretta, R. Nath, M. Moscardini, M. Baenitz, and C. Geibel, Phys. Rev. B **83**, 014412 (2011).

[44] P. Gaveau, J. P. Boucher, L. P. Regnault, and Y. Henry, J. Appl. Phys. **69**, 6228 (1991).

[45] P. C. Hohenberg and B. I. Halperin, Rev. Mod. Phys. **49**, 435 (1977).

[46] M. Campostrini, M. Hasenbusch, A. Pelissetto, P. Rossi, and E. Vicari, Phys. Rev. B **65**, 144520 (2002).

[47] A. W. Sandvik, Phys. Rev. Lett. **80**, 5196 (1998).

[48] D. R. Nelson and J. M. Kosterlitz, Phys. Rev. Lett. **39**, 1201 (1977).

[49] M. S. Makivić, Phys. Rev. B **46**, 3167 (1992).

[50] H.-Q. Ding, Phys. Rev. B **45**, 230 (1992).

[51] We note that a constant was added in the fits to account for the paramagnetic contribution to $1/T_1$.

[52] See Supplemental Material at http://link.aps.org/supplemental/10.1103/PhysRevLett.130.086704 for additional information about the staggered spin correlations investigated by means of NMR, μ^+SR, and QMC, as well as an estimate of the field-induced exchange anisotropy, which includes Refs. [53–61].

[53] J. Als-Nielsen, S. T. Bramwell, M. T. Hutchings, G. J. McIntyre, and D. Visser, J. Phys. Condens. Matter **5**, 7871 (1993).

[54] S. V. Isakov and R. Moessner, Phys. Rev. B **68**, 104409 (2003).

[55] S. T. Bramwell and P. C. W. Holdsworth, J. Phys. Condens. Matter **5**, L53 (1993).

[56] S. T. Bramwell and P. C. W. Holdsworth, Phys. Rev. B **49**, 8811 (1994).

[57] A. Taroni, S. T. Bramwell, and P. C. W. Holdsworth, J. Phys. Condens. Matter **20**, 275233 (2008).

[58] M. Troyer, M. Imada, and K. Ueda, J. Phys. Soc. Jpn. **66**, 2957 (1997).

[59] J.-K. Kim and M. Troyer, Phys. Rev. Lett. **80**, 2705 (1998).

[60] M. Troyer, Universality in two-dimensional quantum Heisenberg antiferromagnets, in *Open Problems in Strongly Correlated Electron Systems*, edited by J. Bonča, P. Prelovšek, A. Ramšak, and S. Sarkar, NATO Science Series Vol. 15 (Springer, Dordrecht, 2001).

[61] P. Hasenfratz and F. Niedermayer, Phys. Lett. B **268**, 231 (1991).

[62] A. Cuccoli, T. Roscilde, V. Tognetti, R. Vaia, and P. Verrucchi, Phys. Rev. B **67**, 104414 (2003).

[63] O. F. Syljuåsen and A. W. Sandvik, Phys. Rev. E **66**, 046701 (2002).

[64] Y.-D. Hsieh, Y.-J. Kao, and A. W. Sandvik, J. Stat. Mech. (2013) P09001.

[65] A. W. Sandvik, AIP Conf. Proc. **1297**, 135 (2010).

[66] D. J. Luitz, F. Alet, and N. Laflorencie, Phys. Rev. B **89**, 165106 (2014).

[67] K. Yosida, *Theory of Magnetism* (Springer-Verlag, Berlin, Heidelberg, 1996).

[68] https://wrap.warwick.ac.uk/139957.

[69] B. Bauer *et al.*, J. Stat. Mech. (2011) P05001.